Regular Article

blood

IMMUNOBIOLOGY AND IMMUNOTHERAPY

A critical epithelial survival axis regulated by MCL-1 maintains thymic function in mice

Reema Jain,[1,2] Julie M. Sheridan,[1,2] Antonia Policheni,[1,2] Melanie Heinlein,[1,2] Luke C. Gandolfo,[1,3] Grant Dewson,[1,2] Gordon K. Smyth,[1,3] Stephen N. Sansom,[4] Nai Yang Fu,[5,6] Jane E. Visvader,[1,2] Georg A. Holländer,[7] Andreas Strasser,[1,2] and Daniel H. D. Gray[1,2]

[1]Walter and Eliza Hall Institute of Medical Research, Melbourne, VIC, Australia; [2]Department of Medical Biology and [3]School of Mathematics and Statistics, University of Melbourne, Melbourne, VIC, Australia; [4]Kennedy Institute of Rheumatology, University of Oxford, Oxford, United Kingdom; [5]Programme in Cancer and Stem Cell Biology, Duke-NUS Medical School, Singapore; [6]Biology Department, College of Science, Shantou University, Shantou, China; and [7]Weatherall Institute for Molecular Medicine, University of Oxford, Oxford, United Kingdom

Key Points

- MCL-1 is essential, but BCL-2 and BCL-XL are dispensable, for TEC survival and thymic function.
- Epidermal growth factor upregulates MCL-1 in TECs.

T-cell differentiation is governed by interactions with thymic epithelial cells (TECs) and defects in this process undermine immune function and tolerance. To uncover new strategies to restore thymic function and adaptive immunity in immunodeficiency, we sought to determine the molecular mechanisms that control life and death decisions in TECs. Guided by gene expression profiling, we created mouse models that specifically deleted prosurvival genes in TECs. We found that although BCL-2 and BCL-XL were dispensable for TEC homeostasis, MCL-1 deficiency impacted on TECs as early as embryonic day 15.5, resulting in early thymic atrophy and T-cell lymphopenia, with near complete loss of thymic tissue by 2 months of age. MCL-1 was not necessary for TEC differentiation but was continually required for the survival of mature cortical and medullary TECs and the maintenance of thymic architecture. A screen of TEC trophic factors in organ cultures showed that epidermal growth factor upregulated MCL-1 via MAPK/ERK kinase activity, providing a molecular mechanism for the support of TEC survival. This signaling axis governing TEC survival and thymic function represents a new target for strategies for thymic protection and regeneration. (*Blood*. 2017;130(23):2504-2515)

Introduction

Thymic epithelial cells (TECs) are an integral part of the thymic microenvironment and are essential for all major steps in thymocyte differentiation. The cortical epithelium drives commitment of hematopoietic precursors to the T-cell lineage, their proliferation, and the positive selection of thymocytes with potentially useful T-cell receptors (TCRs).[1] Medullary TECs (mTECs) are essential for negative selection and regulatory T (Treg) cell development, in part because of their expression of the autoimmune regulator (AIRE).[2] Numerous studies have revealed that defects in TEC differentiation can, in turn, perturb T-cell differentiation to cause immunodeficiency or autoimmune disease.[3] Given the importance of TECs for acquired immunity, the molecular mechanisms that govern their generation and function have been a major focus in the field, with a view to developing strategies to improve or restore thymic function in immunocompromised patients.[4,5] These mechanisms are likely to be highly dynamic. The TEC compartment exhibits a high rate of proliferation and is capable of replacement within ~2 weeks in the adult mouse.[6-8] Distinct TEC subsets exhibit differential mitotic rates, a feature that supports the concept that adult TEC homeostasis is maintained by continual proliferation and differentiation of progenitor cells counterbalanced by cell attrition.

TECs in adult mice can be divided into 4 major populations based on location, phenotype, and function: cortical TECs (cTECs), mTECs that express low levels of major histocompatibility complex (MHC) II/CD80 ($mTEC^{low}$), and mTECs that express high levels of MHC II/CD80 that can be divided into $AIRE^{+}mTEC^{high}$ and $AIRE^{-}mTEC^{high}$. The $mTEC^{low}$ subset has a low proliferative rate and includes at least some progenitors of $mTEC^{high}$.[7-10] The greatest levels of proliferation have been observed in $mTEC^{high}$, particularly in the $AIRE^{-}$ subset.[7-9] It is currently unclear how TECs are lost, and few studies have considered the mechanisms controlling attrition. AIRE expression can lead to heightened apoptosis in vitro[8,11,12]; however, fate-mapping studies indicate that at least some TECs survive AIRE expression in vivo and downregulate this transcriptional regulator.[13,14] Therefore, although we can infer the rate of TEC loss required to counterbalance their high rate of proliferation; the mechanisms, sequence, and contribution of TEC death to thymic function remain unknown.

The intrinsic pathway of apoptosis (also called the mitochondrial, stress-induced, or BCL-2 regulated pathway) is necessary for embryogenesis, deletion of autoreactive lymphocytes, and tissue homeostasis.[15] Disruption of the mitochondrial outer membrane represents the "point of no return" in the intrinsic pathway of apoptosis and is strictly

Submitted 3 March 2017; accepted 21 September 2017. Prepublished online as *Blood* First Edition paper, 29 September 2017; DOI 10.1182/blood-2017-03-771576.

The online version of this article contains a data supplement.

There is an Inside *Blood* Commentary on this article in this issue.

The publication costs of this article were defrayed in part by page charge payment. Therefore, and solely to indicate this fact, this article is hereby marked "advertisement" in accordance with 18 USC section 1734.

regulated via interactions among more than 20 members of the BCL-2 family of proteins. These proteins can be divided into 3 functional factions: (1) the proapoptotic BH3-only proteins, (2) the prosurvival proteins, and (3) the effector proteins, BAX and BAK (and perhaps BOK).[15] In healthy cells, the prosurvival proteins BCL-2, BCL-XL, MCL-1, BCL-W, and BFL-1/A1 prevent BAX and BAK activation and apoptosis. However, cytotoxic stressors can upregulate or activate proapoptotic BH3-only proteins (BIM, PUMA, NOXA, BID, BAD, BIK, HRK, and BMF), which sequester prosurvival proteins and/or directly activate BAX and BAK to trigger apoptosis. Different cell types respond to cytotoxic stimuli with varying sensitivity because the expression and regulation of the BCL-2 family of proteins differ greatly.[15] This variation precludes the prediction of how cells will respond to stress but also creates opportunities for tissue-specific targeting of survival and death proteins for therapeutic benefit.[16,17] In this study, we aimed to understand the molecular pathways that control TEC survival and thymic function. Surprisingly, we found that BCL-2 and BCL-XL were dispensable for TEC survival; however, MCL-1 was essential for the maintenance of specific TEC subsets. We found that epidermal growth factor (EGF) is a positive regulator of this prosurvival protein in TECs, identifying MCL-1 as a tractable target for the amelioration of age- or damage-induced thymic atrophy.

Methods

Mice

Mcl1$^{lox/lox}$,[18] *Bclx*$_L$ $^{lox/lox}$,[19] *Bcl2*$^{lox/lox}$,[20] *Rosa*^{CreERT2}*Mcl1*$^{lox/lox}$,[21] *Foxn1*^{Cre},[22] *Bak*$^{-/-}$,[23] *Bax*$^{lox/lox}$,[24] *Aire*$^{GFP/+}$, and *Aire*$^{-/-}$[25] mice were either generated and maintained on a C57BL/6 background or had been generated on a mixed 129/C57BL/6 background and then backcrossed at least 10 times to C57BL/6 background (except mice that were backcrossed 6 times). The *Mcl1*$^{\Delta K5}$ mice were on a mixed FVB/C57BL/6 background.[26] The *Foxn1*$^{Cre/+}$*Mcl1*$^{lox/-}$ mice were generated by crossing *Mcl1*$^{+/-}$ males[21] with *Mcl1*$^{\Delta Foxn1}$ or *Foxn1*$^{Cre/+}$*Mcl1*$^{lox/+}$ females.

All mice were raised under specific pathogen-free housing conditions according to the regulations of the Walter and Eliza Hall Institute of Medical Research, the Swiss Federal Government, and the Weatherall Institute of Molecular Medicine. All animal experiments were composed of 3 or more mice (unless otherwise stated) in both control and experimental groups and included age-matched controls.

Thymus digestion

Thymi were digested individually as previously described.[27] Briefly, connective tissue was removed, and the 2 thymic lobes were separated. Several snips were made in each lobe with surgical scissors, and the fragments agitated in 5 mL of RPMI-1640 with 25.96 mM *N*-2-hydroxyethylpiperazine-*N*′-2-ethanesulfonic acid with a wide-bore pipette tip. The supernatant was replaced by 1 mL of digestion buffer (RPMI *N*-2-hydroxyethylpiperazine-*N*′-2-ethanesulfonic acid supplemented with Liberase TM [Roche] at 0.5 Wunsch units [U] per mL and DNase I at 0.1% weight-to-volume ratio [Sigma-Aldrich]), and thymic tissue was then digested at 37°C for 15 minutes with gentle agitation every 5 minutes. At the end of the first digestion, the supernatant was recovered and replaced with 500 μL of digestion buffer. Digestion was repeated for 15 minutes at 37°C with gentle agitation after every 5 minutes.

Antibodies and flow cytometry

Surface staining of TECs was performed using the following antibodies that were made at the Walter and Eliza Hall Institute, unless otherwise stated. Anti-mouse CD16/32 FcR-block (clone 2.4G2), anti-mouse CD45 PerCP/Cy5.5 (clone 30-F11, Biolegend), anti-mouse CD31 PerCP/Cy5.5 (clone 390, Biolegend), anti-mouse Ter119 PerCP/Cy5.5 (clone TER119, Biolegend), anti-mouse CD326 (EPCAM) APC/Cy7 (clone G8.8, Biolegend), anti-mouse H-2K^b Pacific Blue (Clone AF6-88.5, Biolegend), anti-H2-A/E fluorescein isothiocyanate (FITC) or allophycocyanin (APC) (clone M5/114.15.2), anti-H2-A/E BV421 (clone M5/114.15.2, Biolegend), biotinylated UEA-1 lectin (Vector labs, USA), anti-mouse Ly51 phycoerythrin (PE) or FITC (clone 6C3, Biolegend), biotinylated anti-mouse CD40 (clone FGK45.5), CD80 BV421 (clone 16-10A1, Biolegend), and anti-human CD4 PE (clone OKT4). Second step staining with streptavidin PE/Cy7 (BD Biosciences) was used to detect biotinylated UEA1 (Vector Laboratories). Propidium iodide or 4′,6-diamidino-2-phenylindole at a final concentration of 2.5 μg/mL was added to samples just prior to data acquisition to label dead cells. Intracellular staining with anti-human Ki67 FITC (clone MOPC-21, BD Pharmingen), anti-mouse AIRE FITC (clone 5H12), anti-mouse β5t (MBL), anti-mouse BCL-2 PE (clone BCL/10C4, Biolegend), anti-mouse BCL-XL (clone E18, Abcam), and anti-mouse MCL-1 Alexa 647 (clone AA3[28]) was performed after fixation and permeabilization with the eBioscience FoxP3 kit.

Lymphocytes were stained using the following antibodies: anti-mouse CD4 APC (clone H129), anti-mouse CD4 PerCP/Cy5.5 (GK1.5, Biolegend), anti-mouse TCRβ PE/Cy7 (H57.59.1, Biolegend), anti-mouse CD8 APC/Cy7 or BV650 (clone 53-6.7, Biolegend), anti-mouse CD25 PE or BV510 (clone PC61, Biolegend), anti-mouse CD44 PE or FITC (clone IM781), and anti-mouse CD62L APC/Cy7 (clone MEL-14, Biolegend). The immature thymocyte depletion cocktail contained biotinylated antibodies against mouse NK1.1 (clone PK136, Biolegend), TER119 (TER119), GR1 (clone RB6-8C5), Mac-1 (clone M1-170), and B220 (RA3-6B2). Second step labeling with streptavidin BV786 (Biolegend) was used to detect the biotinylated antibodies. Screening of the TCRVβ repertoire in the CD4$^+$ and CD8$^+$ populations was analyzed using the Mouse Vβ TCR Screening Panel (BD Pharmingen) antibodies. Intracellular staining using anti-mouse FOXP3 eFluor-450 (clone FJK-165, eBioscience) was performed after fixation and permealization with eBioscience FOXP3 kit. Samples were either acquired, enriched, or sorted using a Fortessa X20 analyzer (BD Biosciences), LSR II (BD Bioscience), AutoMACS (Miltenyi Biotec), and Moflo Legacy (Beckon Coulter). Fluorescence-activated cell sorter data were analyzed using FlowJo software 9.9 (TreeStar).

Immunohistology

Adult (2-month-old) and neonatal (day 9) thymi were isolated, embedded in Tissue-Tek O.C.T. compound (Sakura Finetek), and snap frozen in a liquid nitrogen/isopentane slurry. Sections of 5 to 8 μm were cut using a Microm HM550 Cryostat (Thermo Scientific). Sections were air-dried for 20 minutes and stored at −80°C prior to staining. Sections were blocked with 5% (volume-to-volume ratio) goat serum in phosphate-buffered saline with 0.5% Tween-20 (volume-to-volume ratio) for 30 minutes at room temperature before incubation with primary antibodies for 30 minutes. Primary antibodies included biotinylated anti-mouse pan-keratin (clone Lu-5, LifeSpan BioSciences), anti-mouse K5 (clone Poly 19055, Covance), biotinylated UEA-1 lectin (Vector Labs), anti-mouse DEC205-FITC (clone NLDC145) and anti-mouse AIRE-Alexa647 (clone 5H12), anti-mouse K8 (clone TROMA-I, Developmental Studies Hybridoma Bank [DSHB]) and ER-TR7 (provided by Richard Boyd, Monash University). Following 3 washes in phosphate-buffered saline, 5 minutes each, sections were then incubated with appropriate secondary antibody (anti-rabbit Ig Alexa-555, Life Technologies) and streptavidin FITC (Invitrogen) for 30 minutes, counterstained with 4′,6-diamidino-2-phenylindole (Sigma-Aldrich), then mounted with Vectashield (Vector Labs). Images were collected using a LSM780 confocal with Zen 2012 SP2 (black) software v11.0 (Zeiss). Single optical sections and maximal intensity projection images were processed for presentation using OMERO.[29]

Renal capsule grafting of *Rosa*^{CreERT2}*Mcl1*$^{lox/lox}$ fetal thymus

Thymic lobes were dissected from embryonic day 15.5 (E15.5) embryos and cultured for 2 days in fetal thymic organ culture (FTOC) medium. One lobe from control (*Rosa*^{CreERT2}*Mcl1*$^{+/+}$ or *Rosa*$^{+/+}$*Mcl1*$^{lox/lox}$) and 1 lobe from experimental (*Rosa*^{CreERT2}*Mcl1*$^{lox/lox}$) were transplanted under the renal capsule of the recipient C57BL/6 Ly5.1 males at the anterior and posterior poles of the kidney, respectively. Grafts were allowed to reconstitute for 4 to 8 weeks, then

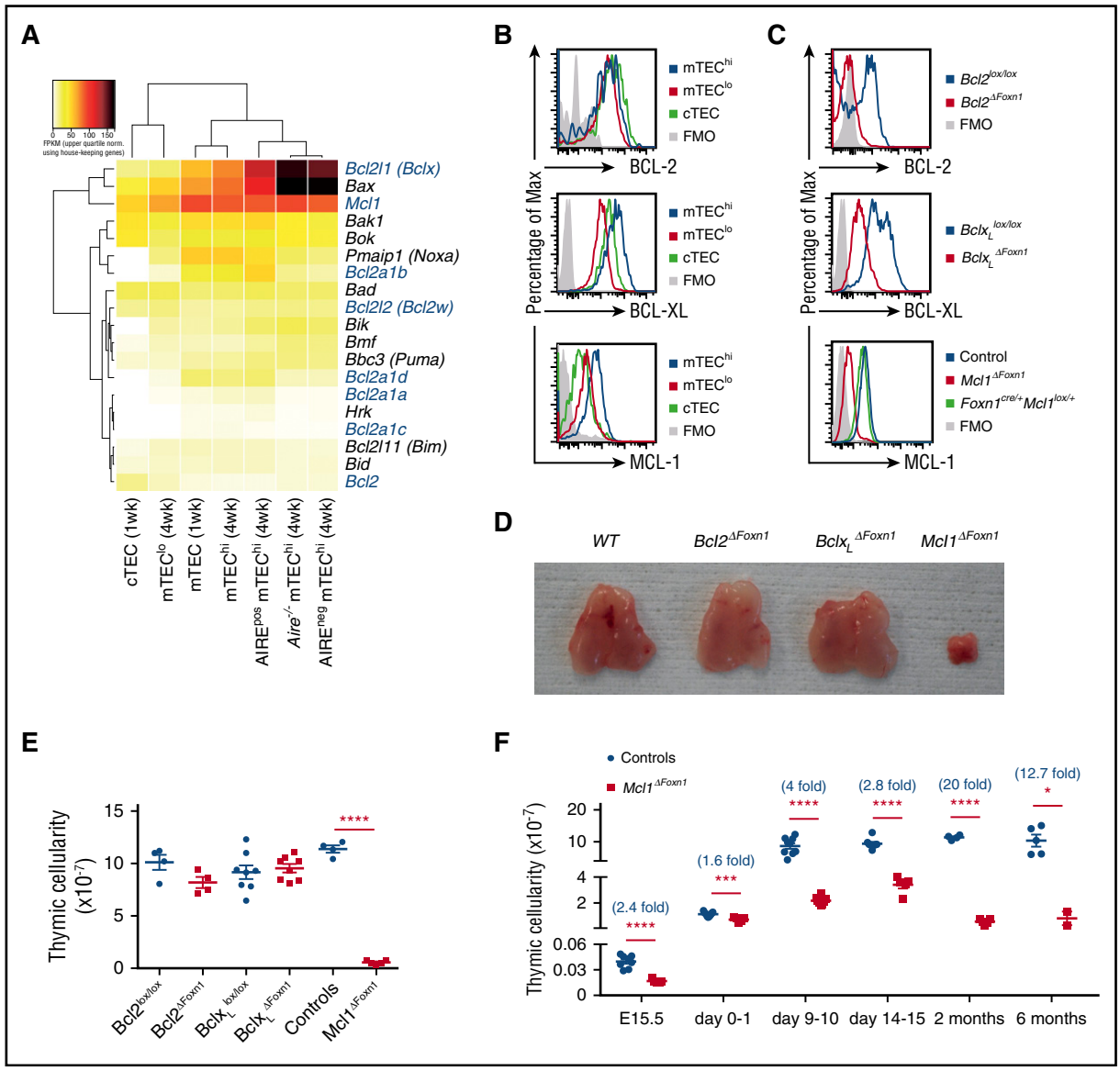

Figure 1. Loss of MCL-1 in TEC precipitates thymic hypoplasia. (A) Heat map of BCL-2 family member expression in the indicated TEC subsets from 1- or 4-week-old wild-type (WT) or *Aire*$^{-/-}$ mice as assessed by RNA sequencing (n = 2). TEC subsets and genes are hierarchically clustered by Pearson correlation and Euclidean distance, respectively. Genes encoding prosurvival proteins are highlighted in blue. (B) Histograms of flow cytometric analysis of BCL-2 (top), BCL-XL (middle), and MCL-1 levels (bottom) in TEC subsets from 2-month-old WT mice. (C) Histograms of flow cytometric analysis of BCL-2 (top), BCL-XL (middle), and MCL-1 (bottom) expression in CD45^{-} EpCAM^{+}MHC II^{+} TECs isolated from day 9, 1 month, and E15.5 embryos, respectively, of the indicated genotypes. (D) Pictures of thymi from 2-month-old female mice of the indicated genotypes. (E) Thymic cellularity of 2-month-old mice of the indicated genotypes. (F) Thymic cellularity of controls (blue circles) and *Mcl1*$^{\Delta Foxn1}$ (red squares) mice at various ages. The numbers in parentheses indicate the mean fold change in thymic cellularity (controls/*Mcl1*$^{\Delta Foxn1}$ mice). Data representative of at least 2 independent experiments are shown. Graph bars indicate mean ± standard error of the mean (SEM), and groups were compared with a Student *t* test (2 sided, unpaired). *$P < .05$; **$P < .01$; ***$P < .001$; ****$P < .0001$. The control group includes various combinations of genotypes (*Foxn1*$^{Cre/+}$*Mcl1*$^{+/+}$, *Foxn1*$^{+/+}$*Mcl1*$^{lox/+}$, *Foxn1*$^{+/+}$*Mcl1*$^{lox/lox}$, *Foxn1*$^{Cre/+}$*Mcl1*$^{lox/+}$) that showed no differences from each other in separate experiments (n ≥ 3/group). FMO, fluorescence minus one.

mice were orally gavaged with 200 mg tamoxifen/kg (Sigma-Aldrich) in peanut oil/10% ethanol for 3 alternate days and were then analyzed at 2 months, 1 month, or 5 days after the third dose.

Data analysis

Statistical analyses were performed using Prism version 6. Outliers were not excluded in any of the experiments. Experiments containing 3 or more groups were analyzed using analysis of variance followed by a Tukey's post hoc test. Experiments with 2 groups were analyzed with 2-tailed Student *t* test. *P* values <.05 were considered as the threshold for statistical significance for all statistical tests. RNA-sequencing (Figure 1A) reads from (Gene Expression Omnibus database accession number GSE53110)[25] were remapped with Hisat2[30] against the mouse genome (mm10) before quantitation of Ensembl 83 genes with Cufflinks.[31] Intersample normalization was performed with the upper quartile method based on housekeeping gene[32] expression.

Results

Differential expression and requirement for BCL-2 family members among TEC subsets

To determine the transcriptional profiles of BCL-2 family genes in TECs, we analyzed RNA sequence data from TEC subsets.[25] We found

that *Bcl2, Bcl2l1* (encoding BCL-XL; hereafter referred to as $Bclx_L$), and *Mcl1* were differentially expressed among the major TEC subsets (Figure 1A), with evidence of high coexpression of $Bclx_L$ and *Mcl1* in mTEC populations. These data were supported by intracellular flow cytometric analysis that revealed similar levels of BCL-2 throughout TEC subsets and the highest levels of BCL-XL and MCL-1 in $mTEC^{hi}$ (Figure 1B). In order to investigate the functional importance of these proteins during TEC development and homeostasis, we deleted these genes only in TECs by crossing $Foxn1^{Cre}$ transgenic mice[22] with mice bearing *loxP* flanked *Bcl2*,[20] $Bclx_L$,19 or *Mcl1*.[18] Efficient and early TEC-specific deletion of these prosurvival genes was confirmed by flow cytometry and western blotting, with at least 90% of TECs deleting the respective genes as early as E13.5 (Figure 1C; supplemental Figure 1A-C, available on the *Blood* Web site).

TEC-specific deletion of $Bclx_L$ ($Bclx_L^{\Delta Foxn1}$) or *Bcl2* ($Bcl2^{\Delta Foxn1}$) did not cause gross thymic abnormalities in 2-month-old adult mice (Figure 1D-E). By contrast, TEC-specific loss of *Mcl1* ($Mcl1^{\Delta Foxn1}$) induced marked thymic hypoplasia in adult mice (Figure 1D-E). Analysis of thymic ontogeny in $Mcl1^{\Delta Foxn1}$ mice revealed decreased thymic cellularity as early as E15.5 compared with controls (Figure 1F). This defect worsened with age, such that 2-month-old mice exhibited ~20-fold lower thymic cellularity compared with controls (Figure 1F). These data show that MCL-1 expression by TECs is essential for normal thymic development and homeostasis.

Impaired thymocyte differentiation and T-cell lymphopenia in $Mcl1^{\Delta Foxn1}$ mice

To test the function of the hypotrophic thymi in $Mcl1^{\Delta Foxn1}$ mice, we analyzed thymocyte differentiation in young (day 9) and adult (2-month-old) $Mcl1^{\Delta Foxn1}$ mice. Populations of $CD4^-CD8^-$ double negative (DN), $CD4^+CD8^+$ double positive (DP), and $CD4^+CD8^-$ and $CD4^-CD8^+$ single positive thymocytes were present, indicating some level of T-cell differentiation in $Mcl1^{\Delta Foxn1}$ mice (Figure 2A; supplemental Figure 2A). However, there was a major numerical deficit in all thymocyte subsets from $Mcl1^{\Delta Foxn1}$ mice, particularly DP (Figure 2A). Analysis of the different subsets of immature DN progenitors (DN1, $CD25^-CD44^+$; DN2, $CD25^+CD44^+$; DN3, $CD25^+CD44^-$; DN4, $CD25^-CD44^-$) revealed that all 4 subsets were reduced, with some indication of a partial block in DN3 thymocytes in 2-month-old $Mcl1^{\Delta Foxn1}$ mice (Figure 2A; supplemental Figure 2B). Studies have shown that the number of DP cells is proportional to the number of DN cells in the thymus.[33,34] Therefore, a decrease in DP numbers in $Mcl1^{\Delta Foxn1}$ mice could be a result of the decrease in the number of DN cells or the import of progenitors. Likewise, a decline in the numbers of critical $FOXP3^+$ Treg cells that depend on the medullary microenvironment for their development was observed[35] (Figure 2B).

Consistent with the observed thymocyte deficiency, $Mcl1^{\Delta Foxn1}$ mice had a paucity of peripheral T cells (Figure 3A; supplemental Figure 3A). Although peripheral B-cell numbers were nearly normal, both $CD4^+$ and $CD8^+$ T cells were reduced in day 9 and 2-month-old $Mcl1^{\Delta Foxn1}$ mice (Figure 3A; supplemental Figure 3A-B). This T-cell lymphopenia was most pronounced in the naïve $CD44^{low}CD62L^{high}$ compartment that relies on thymic output[36] (Figure 3B-C; supplemental Figure 3C). Conversely, there was a proportional expansion of T cells with a central/effector memory, regulatory or proliferating ($Ki67^+$) phenotype observed in young and old $Mcl1^{\Delta Foxn1}$ mice (Figure 3B-E; supplemental Figure 3C-E), with evidence of an altered TCR repertoire (supplemental Figure 3F). This outcome likely reflects lymphopenia-induced T-cell expansion in the periphery in response to the deficit in T-cell production by the thymus, with a consequent increase in the bioavailability of homeostatic cytokines, such as interleukin-2 (IL-2) and IL-7. Interestingly, these features, along with lower numbers of Tregs and medullary hypoplasia in neonates, did not result in autoimmunity; we could not detect signs of excessive leukocyte infiltration into tissues of aged $Mcl1^{\Delta Foxn1}$ mice (data not shown).

To address whether the residual thymic tissue observed in $Mcl1^{\Delta Foxn1}$ mice was because of incomplete deletion of all *Mcl1* alleles, we analyzed adult $Foxn1^{cre/+}Mcl1^{lox/-}$ mice. These mice also exhibited severe thymic atrophy and T-cell lymphopenia to a similar extent to $Mcl1^{\Delta Foxn1}$ mice, with some residual thymopoiesis (supplemental Figure 4 and data not shown). Together, these data indicate that the thymic defects in $Mcl1^{\Delta Foxn1}$ mice cause substantial distortion of the peripheral T-cell pool.

MCL-1 is essential for TEC homeostasis

To determine how the loss of MCL-1 in TEC impaired thymic function in $Mcl1^{\Delta Foxn1}$ mice, we carried out a detailed analysis of $CD45^-$ $EpCAM^+MHC\ II^+$ TECs at key time points (*Mcl1* deficiency did not reduce MHC II levels on TECs; data not shown). Flow cytometric analysis revealed that MCL-1 deficiency reduced TEC numbers as early as E15.5 and that this defect was exacerbated with age (Figure 4A). Nevertheless, all major TEC subsets could be recovered from day 9 $Mcl1^{\Delta Foxn1}$, including cTECs, $mTEC^{low}$, $AIRE^-$ $mTEC^{high}$, and $AIRE^+$ $mTEC^{high}$ (Figure 4B-F). However, there was a severe deficiency in mTEC number in day 9 and 2-month-old $Mcl1^{\Delta Foxn1}$ mice that affected both phenotypically immature ($CD80^-$/$MHC\ II^{low}$) and mature ($CD80^+$/$MHC\ II^{high}$) mTECs, including the $AIRE^+$ $mTEC^{high}$ subset that is critical for imposing immune tolerance (Figure 4B-F).[8,10] The proportion of proliferating TECs ($Ki67^+$) was higher in E15.5 and day 9 $Mcl1^{\Delta Foxn1}$ mice (Figure 4G-H), suggesting that either there is a specific loss of nondividing TECs or the remaining population undergoes heightened proliferation to compensate for TEC death caused by the loss of MCL-1. Regardless, these data indicate that MCL-1 is not critical for the differentiation of the major TEC subpopulations but is essential for their maintenance.

TEC-specific MCL-1 deficiency also impacted on the overall thymic architecture. Immunohistological analysis of the thymus from $Mcl1^{\Delta Foxn1}$ mice revealed extensive and progressive disruption of cortical (labeled with anti-keratin-8, anti-DEC205) and medullary regions (labeled with anti-keratin-5 and UEA-1) (Figures 4I-J; supplemental Figure 5A-B). The few small medullary areas containing $AIRE^+$ TECs in $Mcl1^{\Delta Foxn1}$ mice at day 9 were nearly completely absent by 2 months of age (Figure 4K; data not shown), and thymi were heavily populated by $ER\text{-}TR7^+$ thymic fibroblasts (Figure 4L). These data show that TEC-specific MCL-1 deficiency induces near complete loss of mTECs in adult mice, cTEC compositional changes, and the disruption of the entire thymic microenvironment.

Although the cTEC numbers in $Mcl1^{\Delta Foxn1}$ mice were comparable to controls, the early thymocyte defects prompted a deeper analysis of the functional competence of this subset. A multidimensional scaling plot of RNA-sequencing data from fluorescence-activated cell sorter purified TEC subsets from 1-month-old $Mcl1^{\Delta Foxn1}$ and control mice revealed grossly altered gene expression in cTECs, but not mTECs (Figure 5A; data not shown). In particular, the cTEC population in $Mcl1^{\Delta Foxn1}$ mice displayed differential expression of TEC progenitor genes (eg, increased *Foxn1* and *Psmb11* (aka beta5t) and reduced *Plet1*, *Cldn3*, and *Cldn4*) and mediators of early thymocyte differentiation (eg, reduced *Il7*, *Ccl19*, and *Ccl21* and increased *Dll4*), suggesting compositional changes in the absence of MCL-1 that impact on mature cTEC function (Figure 5B). These findings were supported by flow cytometric analysis of β5t, CD40 and MHC I, CD80 on cTECs and TECs, respectively, from $Mcl1^{\Delta Foxn1}$ mice (Figure 5C-F).

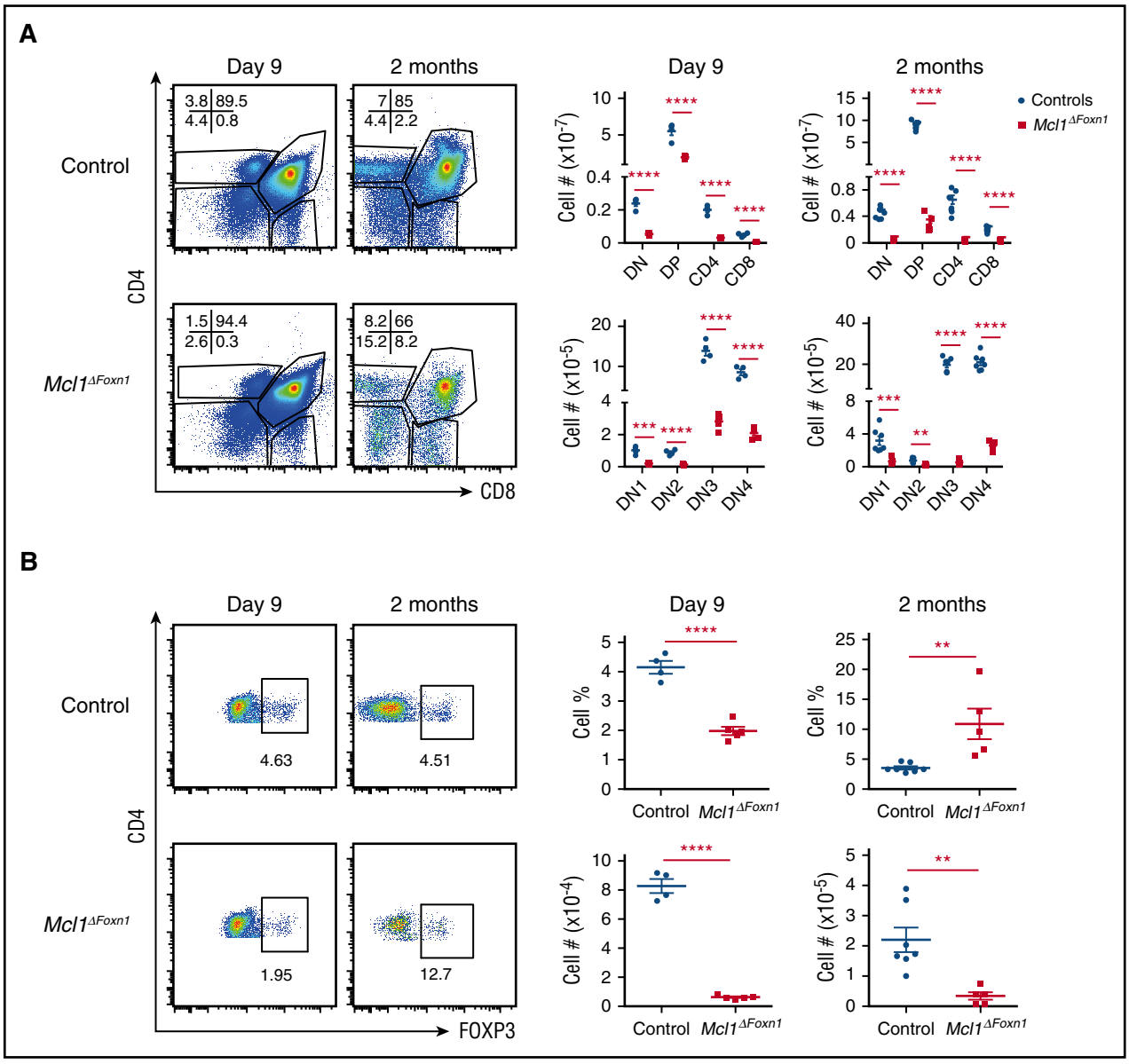

Figure 2. Reduced thymocytes and thymic Foxp3$^+$ Treg cells in *Mcl1$^{\Delta Foxn1}$* mice. (A) Flow cytometry plots of CD4 vs CD8 expression on thymocytes. Graphs represent the numbers of different thymocyte and DN subsets in the thymus. (B) Flow cytometry plots of CD4 vs FOXP3 gated on CD4 single positive thymocytes, with the proportion of cell bounded by regions indicated. Graphs show the proportion and number of thymic FOXP3$^+$ Treg cells from controls and *Mcl1$^{\Delta Foxn1}$* mice at the indicated ages. Data representative of at least 2 independent experiments are shown (except Treg cell data for 2 months). Graph bars indicate mean ± SEM and groups were compared with a Student *t* test (2 sided, unpaired). $^{**}P < .01$; $^{***}P < .001$; $^{****}P < .0001$. The control group combines various combinations of genotypes (*Foxn1$^{Cre/+}$Mcl1$^{+/+}$*, *Foxn1$^{+/+}$Mcl1$^{lox/+}$*, *Foxn1$^{+/+}$Mcl1$^{lox/lox}$*, *Foxn1$^{Cre/+}$Mcl1$^{lox/+}$*) that showed no differences from each other in separate experiments (n ≥ 3/group; where n represents the number of mice per group with each point denoting a mouse).

To test whether MCL-1 was required to antagonize the intrinsic pathway of apoptosis in TECs, we also deleted the key effector proteins BAK and/or BAX in *Mcl1$^{\Delta Foxn1}$* mice. Compound deletion of these genes (or loss of BAK alone) was sufficient to completely rescue thymic atrophy, TEC numbers, composition, and thymus function in *Mcl1$^{\Delta Foxn1}$* mice, indicating that MCL-1 is essential to prevent excessive TEC apoptosis (Figure 5G-H; data not shown).

To verify the requirement for MCL-1 in TEC survival and homeostasis, we used an alternative epithelial-specific Cre transgenic mouse. All TECs express K5 early during development,[37] so we employed a previously published *K5^{Cre}* strain[38] to delete *Mcl1* and found that young *Mcl1$^{\Delta K5}$* mice exhibited thymic atrophy similar to that observed in the *Mcl1$^{\Delta Foxn1}$* mice (supplemental Figure 6A-B). The low numbers of TECs that remained in *Mcl1$^{\Delta K5}$* mice supported residual thymic function and a diminished peripheral T-cell compartment (supplemental Figure 6C-E). Collectively, these data identify an essential role for MCL-1 in maintaining the mature TEC compartment throughout thymus development.

Ongoing requirement for MCL-1 in TEC survival

Is the thymic atrophy in adult *Mcl1$^{\Delta Foxn1}$* and *Mcl1$^{\Delta K5}$* mice caused by the loss of TEC progenitors during development, or is it because of an ongoing requirement for this prosurvival protein for steady-state TEC homeostasis? To address this question, we turned to an inducible deletion system, where ablation of *Mcl1* could be achieved specifically in the thymic stroma after the microenvironment had been fully established. Thymic lobes from E15.5 *Rosa^{CreERT2}Mcl1$^{lox/lox}$* embryos

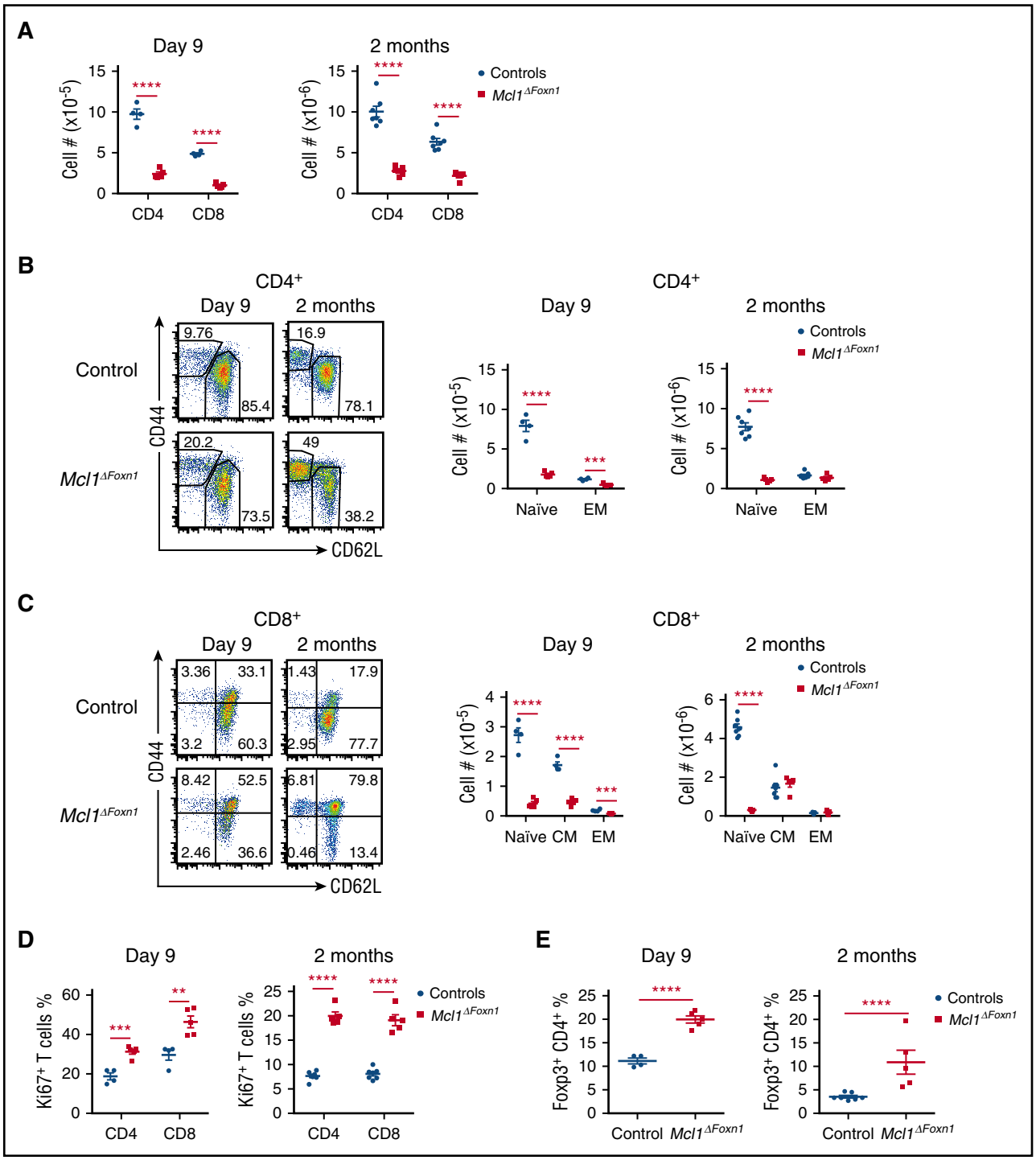

Figure 3. Deficiency in peripheral naïve T cells in *Mcl1*$^{\Delta Foxn1}$ mice. (A) Graphs show the numbers of CD4$^+$ and CD8$^+$ T cells gated on splenic TCRβ$^+$. Flow cytometry plots of CD44 vs CD62L gated on splenic TCRβ$^+$CD4$^+$ (B) or TCRβ$^+$CD8$^+$ (C) T cells. Graphs show the numbers of naïve (CD44^{low}/CD62L^{high}), effector (CD44^{high}/CD62L^{low}), and central memory (CD44^{high}/CD62L^{high}) TCRβ$^+$CD4$^+$ (B) or CD8$^+$ (C) from controls and *Mcl1*$^{\Delta Foxn1}$ mice. (D) Graphs show the proportions of proliferating (Ki67$^+$) CD4$^+$ and CD8$^+$ T cells from controls and *Mcl1*$^{\Delta Foxn1}$ mice at indicated ages. (E) Graphs show the proportions of splenic Treg cells from controls and *Mcl1*$^{\Delta Foxn1}$ mice at the indicated time points. Graph bars indicate mean ± SEM and groups were compared with a Student *t* test (2 sided, unpaired). **P* < .05; ***P* < .01; ****P* < .001; *****P* < .0001. Controls include various combinations of genotypes (*Foxn1*$^{Cre/+}$*Mcl1*$^{+/+}$, *Foxn1*$^{+/+}$*Mcl1*$^{lox/+}$, *Foxn1*$^{+/+}$*Mcl1*$^{lox/lox}$, *Foxn1*$^{Cre/+}$*Mcl1*$^{lox/+}$) that showed no differences from each other in separate experiments (n ≥ 3/group).

were grafted under the renal capsule of C57BL/6-Ly5.1 mice (control lobes without either *Rosa*^{CreERT2} or *loxP* flanked *Mcl1* alleles or heterozygotes were placed on the opposite pole of the kidney). Host hematopoietic cells were allowed to reconstitute between 4 and 8 weeks, and then Cre-ERT2-mediated deletion of *Mcl1* was induced by tamoxifen administration (Figure 6A). We found that thymic grafts from *Rosa*^{CreERT2}*Mcl1*$^{lox/lox}$ lobes could be recovered 5 days following tamoxifen treatment but that substantial loss of TECs had already occurred following deletion of MCL-1 (Figure 6B-D). This loss of TECs apparently induced thymic atrophy because only residual thymic

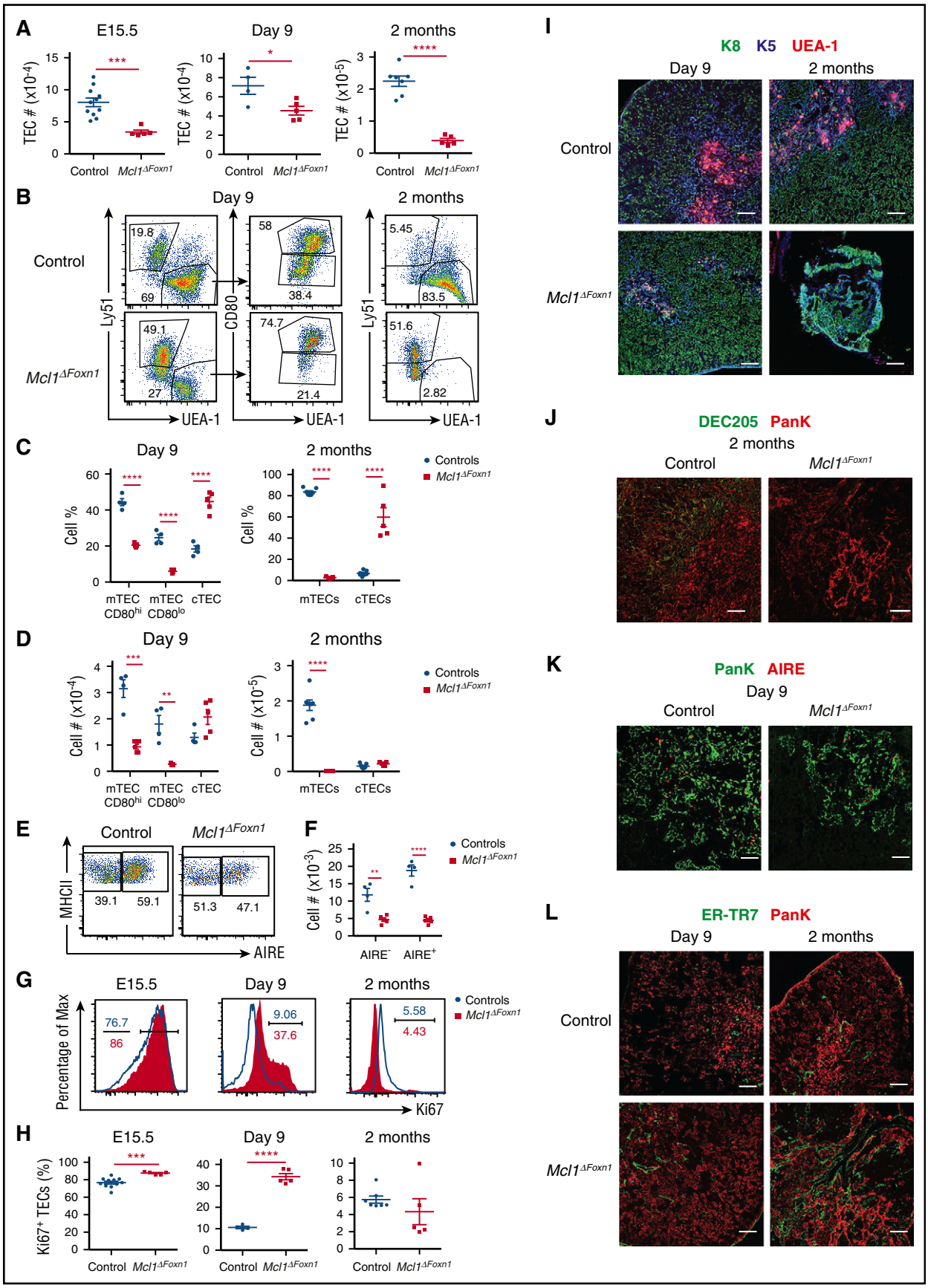

Figure 4. Progressive loss of TECs in *Mcl1*$^{\Delta Foxn1}$ mice. (A) TEC (CD45$^-$MHC II$^+$EpCAM$^+$) numbers from control and *Mcl1*$^{\Delta Foxn1}$ mice at different time points. Representative flow cytometry plots (B) and graphs showing proportions (C) and absolute numbers (D) of cTECs (Ly51$^+$UEA-1$^-$) and CD80$^+$ and CD80$^-$ mTECs or total mTECs (Ly51$^-$UEA-1$^+$). Representative flow cytometry plots (E) and graphs showing absolute numbers (F) of CD80$^+$ mTECs expressing AIRE in day 9 *Mcl1*$^{\Delta Foxn1}$ mice.

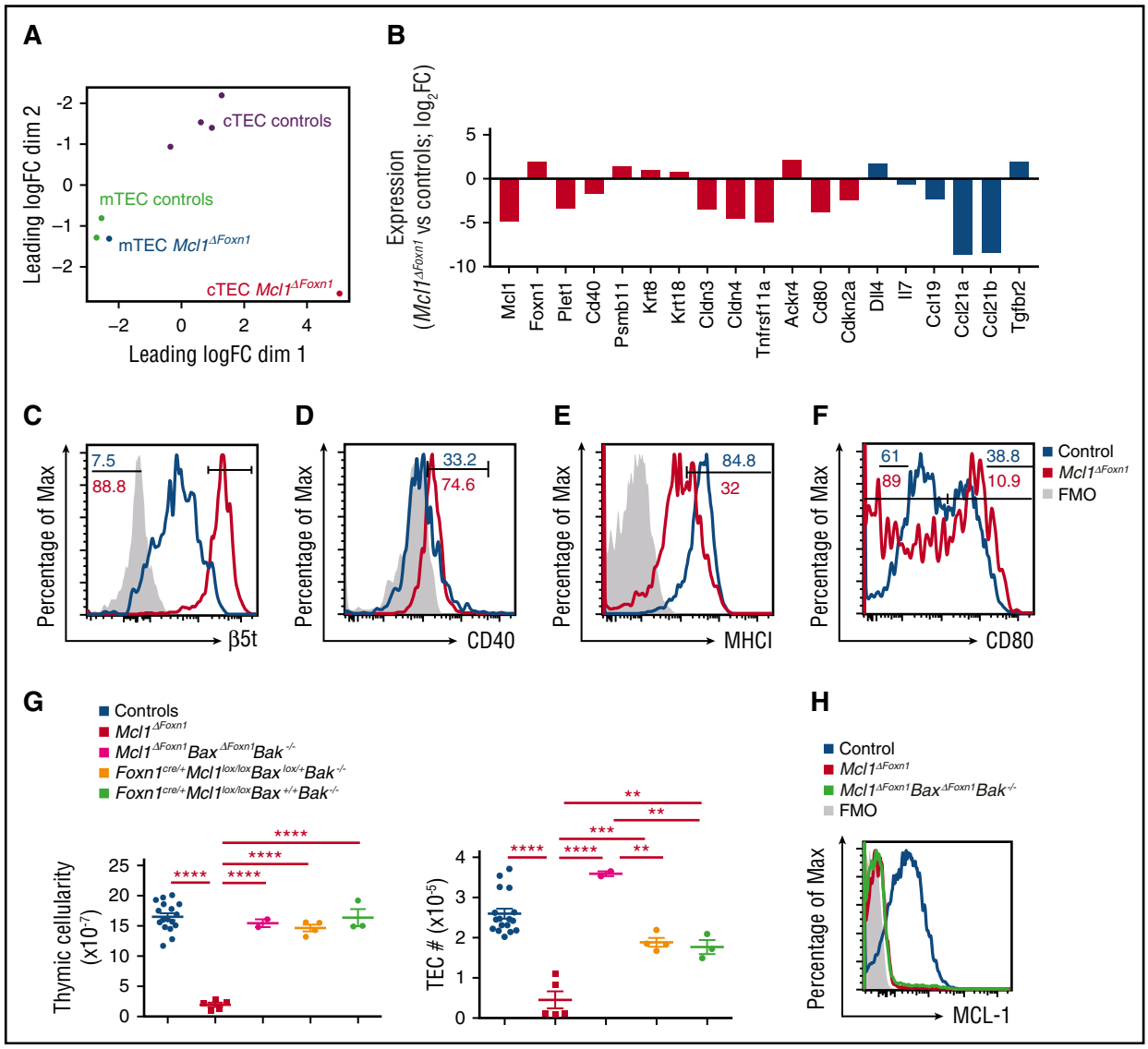

Figure 5. MCL-1 is required for mature TEC survival. (A) Multidimensional scaling plot comparing RNA-sequencing expression profiles for cTECs and mTECs from 1-month-old controls and $Mcl1^{\Delta Foxn1}$ mice. Libraries are labeled and colored according to the genotype and TEC subset. Distances on the plot correspond to leading log 2 fold-change between each pair of samples. (B) Genes that were differentially expressed (false discovery rate < 0.05) in $Mcl1^{\Delta Foxn1}$ cTECs relative to controls that are involved in TEC (red) or thymocyte (blue) development. Histograms of β5t (C), CD40 (D) expression in $CD45^-EpCAM^+MHC\ II^+Ly51^+$ cTECs and MHC I (E), CD80 (F) in $CD45^-EpCAM^+MHC\ II^+$ TECs isolated from 5-week-old mice (blue and red histograms show controls and $Mcl1^{\Delta Foxn1}$ mice, respectively). (G) Thymic cellularity (left) and TEC ($CD45^-MHC\ II^+EpCAM^+$) numbers (right) of 4- to 7-week-old mice of the indicated genotypes. (H) Histogram of flow cytometric analysis of MCL-1 expression in $CD45^-EpCAM^+MHC\ II^+$ TECs isolated from 4- to 7-week-old mice of the indicated genotypes. Data are representative of 3 independent experiments (n ≥ 2/group) (except A-F). Graph bars indicate mean ± SEM and groups were compared with a Student *t* test (2 sided, unpaired). $^{**}P < .01$; $^{***}P < .001$; $^{****}P < .0001$.

tissue could be recovered from $Rosa^{CreERT2}Mcl1^{lox/lox}$ grafts 2 months after treatment, whereas control lobes remained intact (Figure 6B- C). Although the deletion of MCL-1 was not limited to TECs in this model, the extent and kinetics of thymic atrophy observed in this grafting and acute deletion system recapitulated that observed in adult $Mcl1^{\Delta Foxn1}$ mice, supporting the notion that there is an ongoing requirement for MCL-1 for postnatal TEC survival. Furthermore, we found no evidence of selective effects of MCL-1 deletion on $CD45^-EpCAM^-$ nonepithelial stroma (Figure 6D, right), suggesting that the specific loss of TECs we observed following *Mcl1* deletion reflects an ongoing requirement for this prosurvival protein in TEC homeostasis.

EGF regulates MCL-1 expression in TECs

The present data suggest that the mechanisms that regulate MCL-1 expression in TECs are pertinent to thymic function. Because reciprocal

Figure 4 (continued) Representative histograms (blue and red histograms show controls and $Mcl1^{\Delta Foxn1}$ mice, respectively) (G) and graphs showing proportions of proliferating $Ki67^+$ TECs (H). Data are representative of at least 2 independent experiments (n ≥ 3/group) (except TEC subset data for day 9). Graph bars indicate mean ± SEM and groups were compared with a Student *t* test (2 sided, unpaired). $^*P < .05$; $^{**}P < .01$; $^{***}P < .001$; $^{****}P < .0001$. The control group combines various combinations of genotypes ($Foxn1^{Cre/+}Mcl1^{+/+}$, $Foxn1^{+/+}Mcl1^{lox/+}$, $Foxn1^{+/+}Mcl1^{lox/lox}$, $Foxn1^{Cre/+}Mcl1^{lox/+}$) that showed no differences from each other in separate experiments. Immunofluorescence images of thymic sections from day 9 and 2-month-old control and $Mcl1^{\Delta Foxn1}$ mice stained with anti-K8, anti-K5, and UEA-1 (I); anti-DEC205 and anti-PanK (J); anti-PanK and AIRE (K); and ER-TR7 and anti-PanK (L). Scale bars represent 100 μm (I, J, L) and 50 μm (K). PanK, pan-keratin.

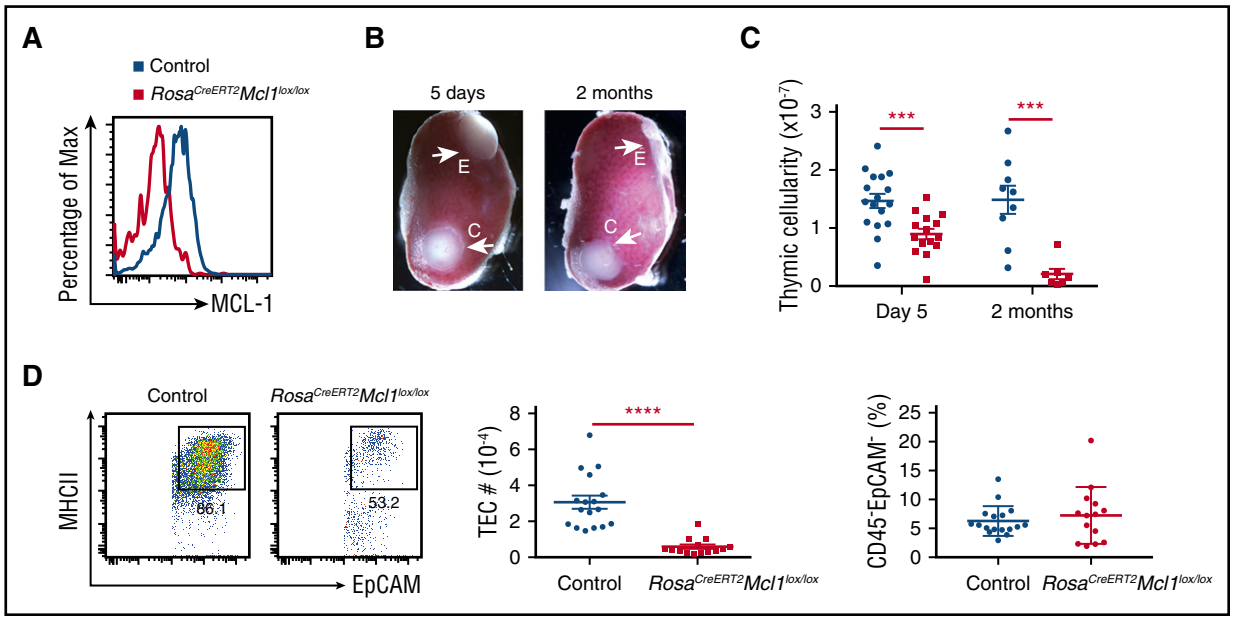

Figure 6. An ongoing requirement for MCL-1 in TEC survival. (A) Representative flow cytometry plots of MCL-1 expression in CD45$^-$EpCAM$^+$MHC II$^+$ TECs isolated from grafts 5 days after the third dose of tamoxifen treatment. (B) Photos of experimental (denoted as "E" for *Rosa*^{CreERT2} *Mcl1*$^{lox/lox}$) and control ("C") thymic lobes grafted under the renal capsule of C57BL/6-Ly5.1 males analyzed at indicated time points after 3 doses of tamoxifen treatment. (C) Total cell numbers recovered from grafts at the indicated time points after third dose of tamoxifen treatment. (D) Flow cytometry plots of MHC II and EpCAM gated on CD45$^-$EpCAM$^+$ TECs (representative of 3 experiments performed on 14-17 mice) and graphs of the number of CD45$^-$EpCAM$^+$MHC II$^+$ TECs (middle) and proportion of CD45$^-$EpCAM$^-$ recovered from grafts 5 days after the third dose of tamoxifen treatment. Bars indicate mean ± SEM and groups were compared with a Student *t* test (2 sided, unpaired). ***$P < .001$; ****$P < .0001$. Controls include various combinations of genotypes (*Rosa*$^{Cre/Cre}$*Mcl1*$^{lox/+}$, *Rosa*$^{+/+}$*Mcl1*$^{lox/+}$, *Rosa*$^{+/+}$*Mcl1*$^{lox/lox}$).

interactions between thymocytes and TECs (termed "thymic cross talk") constitute an important axis for TEC development, we first addressed whether thymocytes affect MCL-1 expression by TECs. Thymic lobes from E15.5 mice were cultured for 5 days in FTOC with 2′-deoxyguanosine (2-dGuo) to selectively deplete thymocytes. We found that the depletion of thymocytes did not influence MCL-1 levels in TECs, as measured by intracellular flow cytometry (Figure 7A). We also tested 3 prominent thymocyte-derived TEC growth factors, CD40L, RANKL, or IL-22, as regulators of MCL-1 expression,[39,40] but none of these ligands altered MCL-1 levels in TECs in 2-dGuo cultured thymic lobes (Figure 7B), consistent with the observation that the loss of thymocytes does not alter the levels of MCL-1 protein in TECs.

To identify signals derived from nonhematopoietic cells that regulate MCL-1 levels in TECs, we tested factors that have been demonstrated to support TEC survival, including EGF,[41] fibroblast growth factor 10,[42] and hepatocyte growth factor[43] (Figure 7C). Using the same assay, we found that EGF substantially augmented the levels of MCL-1 in all TECs (Figure 7C). To determine the pathway mediating this activity, we employed well-characterized inhibitors of EGF receptor signaling.[44,45] EGF-mediated MCL-1 upregulation in TECs was completely prevented by the MAPK/extracellular signal-regulated kinase (MEK) inhibitors U0126, PD98059, and PD0325901[45] (Figure 7D). These data show that EGF regulates expression of prosurvival MCL-1 in TECs via the MAPK/extracellular signal-regulated kinase pathway, consistent with the importance of EGF for supporting thymus development.[41,43-45]

Discussion

Our findings reveal several important aspects of the molecular control of TEC survival. Surprisingly, despite substantial expression of BCL-2 and BCL-XL, these prosurvival proteins appear largely dispensable for TEC homeostasis and thymic function. Whether there might be distinct requirements for these prosurvival proteins in thymic protection or recovery from insults, such as chemotherapy or viral infection, warrants further investigation. By contrast, steady-state thymic function relies on MCL-1 expression by TECs. Among the prosurvival BCL-2 family members, MCL-1 is distinguished by strict posttranslational regulatory mechanisms, a high protein turnover, and a critical role in the survival of multiple hematopoietic lineages.[46] However, MCL-1 is by no means a "universal" survival protein. It is dispensable for the survival of megakaryocytes, platelets,[47] monocytes, macrophages,[48,49] and prepubertal mammary epithelium.[26] Moreover, the distinct regulation of MCL-1 expression in hematopoietic cells (mediated by common-γ chain cytokines) and TECs (mediated, at least in part, by EGF) highlights tissue-specific mechanisms that govern the homeostasis of these lineages.

A feature of the thymic defects in *Mcl1*$^{\Delta Foxn1}$ mice was that they became severe only sometime after the perinatal stages. Although the thymus size decreased in E15.5 and day 9 *Mcl1*$^{\Delta Foxn1}$ mice, all of the major TEC subtypes were present and capable of supporting reduced thymocyte differentiation, indicating that TEC differentiation remains intact in *Mcl1*$^{\Delta Foxn1}$ mice. Yet, their survival was not supported as the thymus matured and mTECs were particularly reliant on MCL-1, because this compartment was substantially diminished by day 9 and essentially absent by 2 months of age. In the cortex, the increased proportion of cycling β5t$^+$, K5/K8$^+$, DEC205$^-$, and CD40$^+$ cTECs and impaired production of key thymocyte growth factors indicated the loss of mature cTECs in *Mcl1*$^{\Delta Foxn1}$ mice could be driving the loss of early thymocyte subsets. All of these features were completely rescued by deletion of the proapoptotic effector protein, BAK, demonstrating that MCL-1 is essential for preventing the premature apoptosis of these mature TECs.

Why is there a delay in thymic atrophy following loss of MCL-1 in TECs? It is notable that the timing of medullary collapse and thymic atrophy in *Mcl1*$^{\Delta Foxn1}$ mice corresponds with an apparent switch in

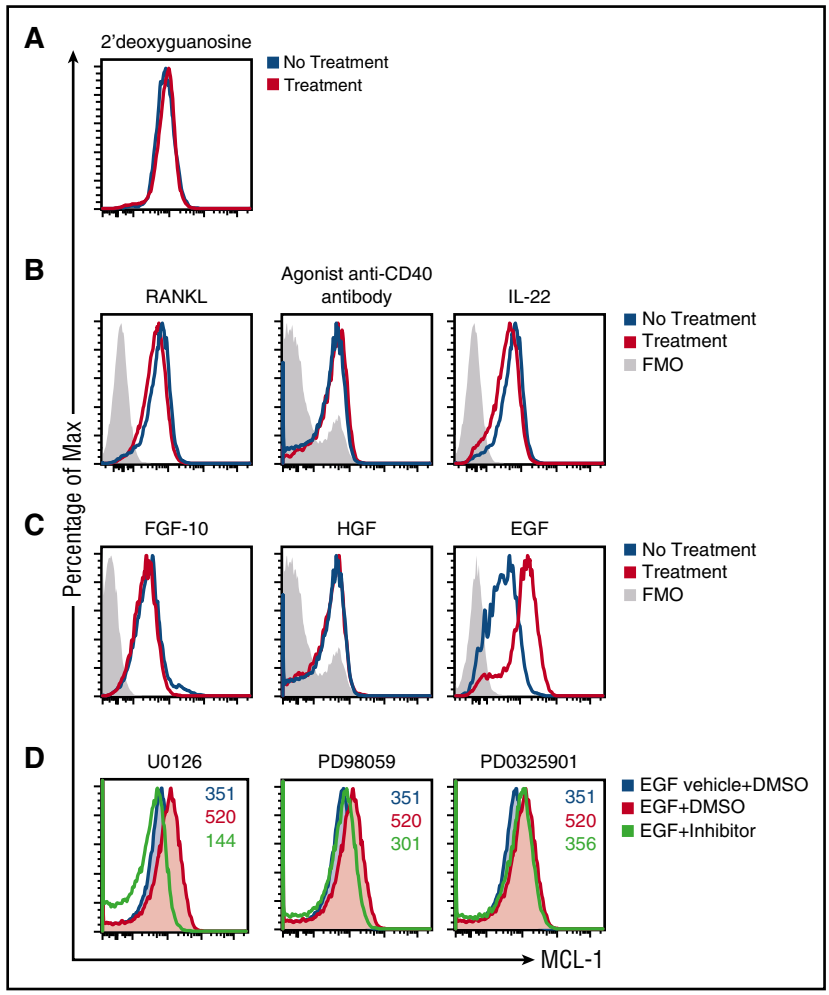

Figure 7. EGF regulates MCL-1 expression in TECs. (A) Histogram of MCL-1 expression in CD45$^-$EpCAM$^+$MHC II$^+$ TECs from FTOC with or without 2-dGuo treatment. Histograms of MCL-1 expression in CD45$^-$EpCAM$^+$MHC II$^+$ TECs from 2-dGuo-FTOC left untreated (blue) or stimulated (red) with RANKL, agonist CD40 antibody, and IL-22 (B); fibroblast growth factor 10 (FGF-10), hepatocyte growth factor (HGF), and EGF (C); EGF+U0126, EGF+PD98059, and EGF+PD0325901 (D). Data are representative of at least 2 experiments with n = 3/treatment. Numbers in panel D plots indicate the geometric mean of the fluorescence intensity. DMSO, dimethyl sulfoxide; IL-22, interleukin-22.

the origin of mTECs. TEC progenitors with a cortical phenotype give rise to a substantial proportion of mTECs early in life; however, this contribution ceases after 1 to 2 weeks, and mTEC-restricted cells maintain the mature medullary compartment.[50] Further investigation of this temporal window in *Mcl1*$^{\Delta Foxn1}$ mice may yield insights into how progenitor cells respond to perturbation of TEC homeostasis caused by loss of differentiated mTECs. For instance, the increased TEC proliferation observed at E15.5 and day 9 is consistent with the notion that elevated bipotent progenitor activity in the cTEC compartment can initially compensate for mature TEC loss in *Mcl1*$^{\Delta Foxn1}$ mice but is unable to maintain this role into adulthood.

Another question raised by these data is whether MCL-1 might drive age-related thymic involution. We could find no significant difference in MCL-1 expression in TECs from 2-month-old vs 1-year-old mice (data not shown), suggesting that this is not the case.

The critical role for MCL-1 in TEC survival raises the question of how the thymic microenvironment regulates this BCL-2 family member in TECs. Among a range of TEC trophic cytokines tested, only EGF positively regulated MCL-1 expression in TECs from 2-dGuo FTOC. Interestingly, TEC expression of EGF receptor is required for proper mTEC number and architecture[43]; however, the extent of these defects is milder than those we observe here, suggesting that there are other regulators of MCL-1 in TECs. In light of these findings, it will be of interest to determine the best strategies for inducing MCL-1 upregulation to support TEC survival in age- or insult-induced thymic atrophy.

The impaired function of the immune system in aged individuals and patients that are unable to restore immune function following thymic insult induced by cancer treatments or infections leads to substantial morbidity and mortality because of higher rates of opportunistic infections, cancer, and autoimmunity.[51-54] Several studies have reported stimulating TEC growth represents a compelling strategy to rejuvenate thymic function in clinical settings.[55-57] Partial regeneration was observed in mice administered with keratinocyte growth factor via the induction of TEC proliferation.[55,58,59] The combined administration of keratinocyte growth factor and an inhibitor of p53, PFT-β, accelerated thymic recovery by restoring TEC numbers after bone marrow transplantation.[56] Our findings indicate that MCL-1 expression is an important biomarker of TEC survival in these contexts. Furthermore, coadministration of factors that target distinct cellular processes in TECs (ie, proliferation and MCL-1-mediated survival) may promote more robust and durable thymic regeneration than has been observed to date.

Acknowledgments

The authors gratefully acknowledge the Gray, Strasser, and Herold labs for valuable feedback. The authors thank the Walter and Eliza Hall Institute Flow Cytometry Laboratory and the Centre for Dynamic Imaging for technical assistance; B. Helbert, K. Mackwell,

and C. Young for mouse genotyping; G. Siciliano, K. Humphreys, S. O'Connor, and H. Marks for animal husbandry; and S. Wilcox, N. Lalaoui, D. Vremec, R. Boyd, A. Chidgey, P. Bouillet, S. Grabow, G. Kelly, B. Kile, I. Tabas, and L. Hennighausen for animals, technical assistance, and/or reagents. TROMA-I was deposited to the DSHB by P. Brulet and R. Kemler (DSHB Hybridoma Product TROMA-I).

This work was supported by grants GNT0637353, GNT1049724, GNT1121325, and GNT1054618 and Career Development Fellowship-2 1090236 (D.H.D.G.), 1016701, Senior Principal Research Fellow Fellowship 1020363 (A.S.), Australia Fellowship (J.E.V.), GNT1086727 (N.Y.F.), and Fellowship 1058892 (G.K.S.) from the Australian National Health and Medical Research Council, Wellcome Trust 105045/Z/14/Z (G.A.H.), the Leukemia & Lymphoma Society of America (Specialized Center of Research grant 7001-13), the Leukaemia Research Foundation, and Melbourne International Research Scholarship and Melbourne International Fee Remission Scholarship (R.J.) from the University of Melbourne. This work was made possible through Victorian State Government Operational Infrastructure Support and Australian Government National Health and Medical Research Council Independent Research Institute Infrastructure Support Scheme.

Authorship

Contribution: R.J., A.S., and D.H.D.G. were responsible for conceptualization; R.J., J.M.S., A.S., and D.H.D.G. developed the methodology; R.J., J.M.S., A.P., M.H., G.K.S., L.C.G., G.D., S.N.S., and D.H.D.G. were responsible for the investigation; S.N.S., N.Y.F., J.E.V., G.A.H., A.S., and D.H.D.G. were responsible for resources; R.J., J.M.S., and D.H.D.G. wrote the original draft of the manuscript; and R.J., J.M.S., G.A.H., A.S., and D.H.D.G. wrote, reviewed, and edited the final manuscript.

Conflict-of-interest disclosure: The authors declare no competing financial interests.

Correspondence: Daniel H. D. Gray, Walter and Eliza Hall Institute of Medical Research, 1G Royal Parade, Parkville, Melbourne, VIC 3052, Australia; e-mail: dgray@wehi.edu.au.

References

1. Ohigashi I, Kozai M, Takahama Y. Development and developmental potential of cortical thymic epithelial cells. *Immunol Rev*. 2016;271(1):10-22.
2. Perry JS, Hsieh CS. Development of T-cell tolerance utilizes both cell-autonomous and cooperative presentation of self-antigen. *Immunol Rev*. 2016;271(1):141-155.
3. Irla M, Hollander G, Reith W. Control of central self-tolerance induction by autoreactive CD4+ thymocytes. *Trends Immunol*. 2010;31(2):71-79.
4. Boehm T, Swann JB. Thymus involution and regeneration: 2 sides of the same coin? *Nat Rev Immunol*. 2013;13(11):831-838.
5. Chaudhry MS, Velardi E, Dudakov JA, van den Brink MR. Thymus: the next (re)generation. *Immunol Rev*. 2016;271(1):56-71.
6. Dumont-Lagacé M, Brochu S, St-Pierre C, Perreault C. Adult thymic epithelium contains nonsenescent label-retaining cells. *J Immunol*. 2014;192(5):2219-2226.
7. Gäbler J, Arnold J, Kyewski B. Promiscuous gene expression and the developmental dynamics of medullary thymic epithelial cells. *Eur J Immunol*. 2007;37(12):3363-3372.
8. Gray D, Abramson J, Benoist C, Mathis D. Proliferative arrest and rapid turnover of thymic epithelial cells expressing Aire. *J Exp Med*. 2007; 204(11):2521-2528.
9. Gray DH, Seach N, Ueno T, et al. Developmental kinetics, turnover, and stimulatory capacity of thymic epithelial cells. *Blood*. 2006;108(12): 3777-3785.
10. Rossi SW, Kim MY, Leibbrandt A, et al. RANK signals from CD4(+)3(-) inducer cells regulate development of Aire-expressing epithelial cells in the thymic medulla. *J Exp Med*. 2007;204(6): 1267-1272.
11. Colomé N, Collado J, Bech-Serra JJ, et al. Increased apoptosis after autoimmune regulator expression in epithelial cells revealed by a combined quantitative proteomics approach. *J Proteome Res*. 2010;9(5):2600-2609.
12. Liiv I, Haljasorg U, Kisand K, Maslovskaja J, Laan M, Peterson P. AIRE-induced apoptosis is associated with nuclear translocation of stress sensor protein GAPDH. *Biochem Biophys Res Commun*. 2012;423(1):32-37.
13. Metzger TC, Khan IS, Gardner JM, et al. Lineage tracing and cell ablation identify a post-Aire-expressing thymic epithelial cell population. *Cell Reports*. 2013;5(1):166-179.
14. Nishikawa Y, Nishijima H, Matsumoto M, et al. Temporal lineage tracing of Aire-expressing cells reveals a requirement for Aire in their maturation program. *J Immunol*. 2014;192(6):2585-2592.
15. Adams JM, Cory S. The Bcl-2 apoptotic switch in cancer development and therapy. *Oncogene*. 2007;26(9):1324-1337.
16. Wang YH, Scadden DT. Harnessing the apoptotic programs in cancer stem-like cells. *EMBO Rep*. 2015;16(9):1084-1098.
17. Anderson MA, Huang D, Roberts A. Targeting BCL2 for the treatment of lymphoid malignancies. *Semin Hematol*. 2014;51(3):219-227.
18. Vikstrom I, Carotta S, Lüthje K, et al. Mcl-1 is essential for germinal center formation and B cell memory. *Science*. 2010;330(6007):1095-1099.
19. Wagner KU, Claudio E, Rucker EB III, et al. Conditional deletion of the Bcl-x gene from erythroid cells results in hemolytic anemia and profound splenomegaly. *Development*. 2000; 127(22):4949-4958.
20. Thorp E, Li Y, Bao L, et al. Brief report: increased apoptosis in advanced atherosclerotic lesions of Apoe-/- mice lacking macrophage Bcl-2. *Arterioscler Thromb Vasc Biol*. 2009;29(2): 169-172.
21. Grabow S, Delbridge AR, Valente LJ, Strasser A. MCL-1 but not BCL-XL is critical for the development and sustained expansion of thymic lymphoma in p53-deficient mice. *Blood*. 2014; 124(26):3939-3946.
22. Zuklys S, Gill J, Keller MP, et al. Stabilized beta-catenin in thymic epithelial cells blocks thymus development and function. *J Immunol*. 2009; 182(5):2997-3007.
23. Lindsten T, Ross AJ, King A, et al. The combined functions of proapoptotic Bcl-2 family members bak and bax are essential for normal development of multiple tissues. *Mol Cell*. 2000;6(6): 1389-1399.
24. Caton ML, Smith-Raska MR, Reizis B. Notch-RBP-J signaling controls the homeostasis of CD8-dendritic cells in the spleen. *J Exp Med*. 2007; 204(7):1653-1664.
25. Sansom SN, Shikama-Dorn N, Zhanybekova S, et al. Population and single-cell genomics reveal the Aire dependency, relief from Polycomb silencing, and distribution of self-antigen expression in thymic epithelia. *Genome Res*. 2014;24(12):1918-1931.
26. Fu NY, Rios AC, Pal B, et al. EGF-mediated induction of Mcl-1 at the switch to lactation is essential for alveolar cell survival. *Nat Cell Biol*. 2015;17(4):365-375.
27. Jain R, Gray DH. Isolation of thymic epithelial cells and analysis by flow cytometry. *Curr Protoc Immunol*. 2014;107:3.26.1-3.26.15.
28. Okamoto T, Coultas L, Metcalf D, et al. Enhanced stability of Mcl1, a prosurvival Bcl2 relative, blunts stress-induced apoptosis, causes male sterility, and promotes tumorigenesis. *Proc Natl Acad Sci USA*. 2014;111(1):261-266.
29. Allan C, Burel JM, Moore J, et al. OMERO: flexible, model-driven data management for experimental biology. *Nat Methods*. 2012;9(3): 245-253.
30. Kim D, Langmead B, Salzberg SL. HISAT: a fast spliced aligner with low memory requirements. *Nat Methods*. 2015;12(4):357-360.
31. Trapnell C, Roberts A, Goff L, et al. Differential gene and transcript expression analysis of RNA-seq experiments with TopHat and Cufflinks. *Nat Protoc*. 2012;7(3):562-578.
32. de Jonge HJ, Fehrmann RS, de Bont ES, et al. Evidence based selection of housekeeping genes. *PLoS One*. 2007;2(9):e898.
33. Almeida AR, Borghans JA, Freitas AA. T cell homeostasis: thymus regeneration and peripheral T cell restoration in mice with a reduced fraction of competent precursors. *J Exp Med*. 2001;194(5): 591-600.
34. Prockop SE, Petrie HT. Regulation of thymus size by competition for stromal niches among early T cell progenitors. *J Immunol*. 2004;173(3): 1604-1611.
35. Cowan JE, Parnell SM, Nakamura K, et al. The thymic medulla is required for Foxp3+ regulatory but not conventional CD4+ thymocyte development. *J Exp Med*. 2013;210(4):675-681.
36. den Braber I, Mugwagwa T, Vrisekoop N, et al. Maintenance of peripheral naive T cells is sustained by thymus output in mice but not humans. *Immunity*. 2012;36(2):288-297.
37. Klug DB, Carter C, Crouch E, Roop D, Conti CJ, Richie ER. Interdependence of cortical thymic epithelial cell differentiation and T-lineage

commitment. *Proc Natl Acad Sci USA*. 1998; 95(20):11822-11827.

38. Tarutani M, Itami S, Okabe M, et al. Tissue-specific knockout of the mouse Pig-a gene reveals important roles for GPI-anchored proteins in skin development. *Proc Natl Acad Sci USA*. 1997;94(14):7400-7405.
39. Akiyama T, Shimo Y, Yanai H, et al. The tumor necrosis factor family receptors RANK and CD40 cooperatively establish the thymic medullary microenvironment and self-tolerance [published correction appears in *Immunity*. 2013;39(4):796]. *Immunity*. 2008;29(3):423-437.
40. Dudakov JA, Hanash AM, Jenq RR, et al. Interleukin-22 drives endogenous thymic regeneration in mice. *Science*. 2012;336(6077): 91-95.
41. Shinohara T, Honjo T. Epidermal growth factor can replace thymic mesenchyme in induction of embryonic thymus morphogenesis in vitro. *Eur J Immunol*. 1996;26(4):747-752.
42. Revest JM, Suniara RK, Kerr K, Owen JJ, Dickson C. Development of the thymus requires signaling through the fibroblast growth factor receptor R2-IIIb. *J Immunol*. 2001;167(4): 1954-1961.
43. Satoh R, Kakugawa K, Yasuda T, et al. Requirement of Stat3 signaling in the postnatal development of thymic medullary epithelial cells. *PLoS Genet*. 2016;12(1):e1005776.
44. Chandra A, Lan S, Zhu J, Siclari VA, Qin L. Epidermal growth factor receptor (EGFR) signaling promotes proliferation and survival in osteoprogenitors by increasing early growth response 2 (EGR2) expression. *J Biol Chem*. 2013;288(28):20488-20498.
45. Leu CM, Chang C, Hu C. Epidermal growth factor (EGF) suppresses staurosporine-induced apoptosis by inducing mcl-1 via the mitogen-activated protein kinase pathway. *Oncogene*. 2000;19(13):1665-1675.
46. Opferman JT. Life and death during hematopoietic differentiation. *Curr Opin Immunol*. 2007;19(5):497-502.
47. Debrincat MA, Josefsson EC, James C, et al. Mcl-1 and Bcl-x(L) coordinately regulate megakaryocyte survival. *Blood*. 2012;119(24): 5850-5858.
48. Dzhagalov I, St John A, He YW. The antiapoptotic protein Mcl-1 is essential for the survival of neutrophils but not macrophages. *Blood*. 2007; 109(4):1620-1626.
49. Steimer DA, Boyd K, Takeuchi O, Fisher JK, Zambetti GP, Opferman JT. Selective roles for antiapoptotic MCL-1 during granulocyte development and macrophage effector function. *Blood*. 2009;113(12):2805-2815.
50. Ohigashi I, Zuklys S, Sakata M, et al. Adult thymic medullary epithelium is maintained and regenerated by lineage-restricted cells rather than bipotent progenitors. *Cell Reports*. 2015;13(7): 1432-1443.
51. Day CL, Kaufmann DE, Kiepiela P, et al. PD-1 expression on HIV-specific T cells is associated with T-cell exhaustion and disease progression. *Nature*. 2006;443(7109):350-354.
52. Douek DC, McFarland RD, Keiser PH, et al. Changes in thymic function with age and during the treatment of HIV infection. *Nature*. 1998; 396(6712):690-695.
53. Douek DC, Vescio RA, Betts MR, et al. Assessment of thymic output in adults after haematopoietic stem-cell transplantation and prediction of T-cell reconstitution. *Lancet*. 2000; 355(9218):1875-1881.
54. Storek J, Gooley T, Witherspoon RP, Sullivan KM, Storb R. Infectious morbidity in long-term survivors of allogeneic marrow transplantation is associated with low CD4 T cell counts. *Am J Hematol*. 1997;54(2):131-138.
55. Alpdogan O, Hubbard VM, Smith OM, et al. Keratinocyte growth factor (KGF) is required for postnatal thymic regeneration. *Blood*. 2006; 107(6):2453-2460.
56. Kelly RM, Goren EM, Taylor PA, et al. Short-term inhibition of p53 combined with keratinocyte growth factor improves thymic epithelial cell recovery and enhances T-cell reconstitution after murine bone marrow transplantation. *Blood*. 2010; 115(5):1088-1097.
57. Kelly RM, Highfill SL, Panoskaltsis-Mortari A, et al. Keratinocyte growth factor and androgen blockade work in concert to protect against conditioning regimen-induced thymic epithelial damage and enhance T-cell reconstitution after murine bone marrow transplantation. *Blood*. 2008; 111(12):5734-5744.
58. Erickson M, Morkowski S, Lehar S, et al. Regulation of thymic epithelium by keratinocyte growth factor. *Blood*. 2002;100(9):3269-3278.
59. Rossi SW, Jeker LT, Ueno T, et al. Keratinocyte growth factor (KGF) enhances postnatal T-cell development via enhancements in proliferation and function of thymic epithelial cells. *Blood*. 2007;109(9):3803-3811.